Acta Technica 63 No. 1B/2018, 1–6

Optimum design and simulation analysis of picking-assist exoskeleton[1]

Lei Yan[2], Shuang Gao[2], Ning Li[23]

Abstract. This work presents a picking-assist exoskeleton with a simple structure to decrease the work intensity of workers performing picking activities outdoors and to avoid fatigue and a prolonged vacant state of the work arm so as to increase work efficiency. Through the optimization calculation of relevant parameters of the crank-slider mechanism, a three-dimensional model of the picking-assist exoskeleton is established using the Solid Edge software and imported into ADAMS for simulation. A comparison of the effects of pre-optimization and post-optimization models verifies the feasibility of the picking-assist exoskeleton for assisting in a work space to complete an operation.

Key words. Picking-assist exoskeleton, crank-slider mechanism, optimization, ADAMS, simulation.

1. Introduction

China is the largest producer and consumer of fruits in the world. With the improvement of people's living standards and the rapid development of fruit cultivation, agricultural picking machinery is now one of the focus areas of research in agricultural machinery [1]. An agricultural mechanism for fruit harvesting is increasingly in demand [2]. In the current situation, the selection of the operating environment is complicated, and seasonality is very strong. A shortage of agricultural workers and high labor costs have prompted the search for mechanical solutions [3]. Moreover, a machine-vision recognition system is expensive and has a low input-output ratio; hence, it cannot be utilized widely. Therefore, there is an urgent need to design a picking-assist exoskeleton to reduce the work intensity of picking workers and improve the picking efficiency, which would be profitable to both producers and consumers [4]. This indicates that the research and utilization of picking-assist

[1]This research is supported by "the Fundamental Research Funds for the Central Universities (No. 2015ZCQ-GX-03).

[2]School of Technology, Beijing Forestry University, Beijing, China

[3]Corresponding author; E-mail: `liningbjfu@163.com`

exoskeletons are significant to improve the degree of picking mechanization. The exoskeleton is a material-handling machine under intimate control of the operator [5]. In November 1965, a research contract for the development of Hardiman I was initiated as a joint army-navy program [6]. The goal of this program was to develop and demonstrate a jointed, load-bearing exoskeleton structure designed to be worn by a person to augment their strength and endurance [5, 7]. Based on the analysis and consideration of all kinds of factors, this work presents a picking-assist exoskeleton with a simple structure that is relatively inexpensive and practical and can be widely used.

2. Method

In August 1990, China began to use the adult male and female human standard GB10000-89. Based on the functional requirements of the human upper arm, the picking-assist exoskeleton designed in this paper can be worn by a picking worker to reduce labor intensity. The mean and standard deviation of dimensions of the human upper arm are listed in Table 1.

Table 1. Size of the human upper arm

Measurement item	Male		Female	
	Mean	Standard deviation	Mean	Standard deviation
Upper-arm length (mm)	313	14.55	284	13.33

The design allows structural picking activities with the range of motion shown in Fig. 1: $\alpha = 15\,^\circ - 165\,^\circ$, $\delta = 15\,^\circ - 165^\circ$.

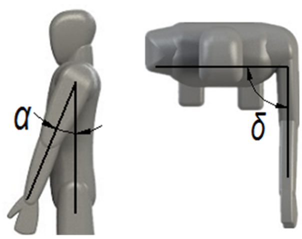

Fig. 1. Range of motion of picking-assist exoskeleton activities

The main movement mechanism of the device is a crank-slider mechanism. In order to determine the position of the picking operation by fixing the position of the slider, the guide rail is designed with a rack shape to achieve follow-up control. The length of the board mounted on the rotating shaft AB can be adjusted according to the size of different people's upper arms. The angle between the connecting rod BC and the slider guide is ϕ. The polar angle is θ. The working angle α is 15°-165°. The allowable transmission angle Υ is 40°. Taking into account the shoulder thickness of the human body, the offset e is not less than 60 mm. Taking into account the distance from the arm to the hip, the length OC is not greater than 300 mm. The sizes of the crank a, connecting rod b, and offset e are determined to design the crank slider mechanism. Let the speed ratio coefficient k be 1.1. The polar angle can be obtained as follows: $\theta = 180 \times \frac{k-1}{k+1} = 8.6°$.

As shown in Fig. 2, when the point passes from point B_2 to point B_0 and moves to point B_1, the working stroke is a fast stroke.

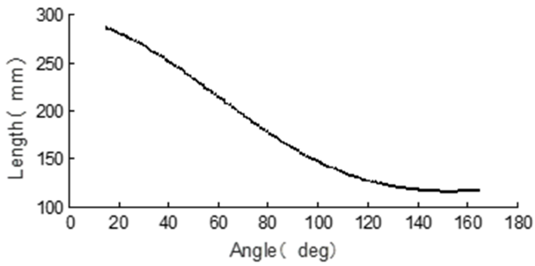

Fig. 2. Variation of length OC with angle β

The minimum transmission angle is derived as

$$\gamma_{\min} = \arccos \frac{a+e}{b} = \arccos \frac{(a+e)/H}{b/H}\,. \tag{1}$$

Through the sine theorem, the following expressions can be derived

$$\frac{a}{H} = \frac{\sin\varphi + \theta - \sin\varphi}{2\sin\theta}\,, \tag{2}$$

$$\frac{b}{H} = \frac{\sin\varphi + \theta) + \sin\varphi}{2\sin\theta}\,, \tag{3}$$

$$\frac{e}{H} = \left(\frac{a}{H} + \frac{b}{H}\right)\sin\varphi\,. \tag{4}$$

The above were substituted into Eq. (1). The minimum transmission angle is thus derived as

$$\gamma_{\min} = \arccos \frac{2\sin(\varphi+\theta)\sin\varphi + \sin(\varphi+\theta) - \sin\varphi}{\sin(\varphi+\theta) + \sin\varphi}\,.$$

From Fig. 2, we can see that, in order to maximize the minimum working stroke, φ and θ should satisfy the following equation:

$$2\sin(\varphi+\theta)\sin\varphi - \sin(\varphi+\theta) + \sin\varphi + \sin(\varphi+\theta)\,[\sin(\varphi+\theta) + \sin\varphi] = 0\,.$$

When θ equals 8.6°, φ equals 6.18°. By substituting θ and φ into (2)–(4), we obtain $\frac{a}{H} = 0.4830\frac{b}{H} = 1.2129\frac{e}{H} = 0.1836$.

Let the slider stroke H be 180 mm. Then, a equals 87 mm, and b equals 218 mm. Considering that the shoulder thickness of the human body, e is not less than 60 mm, we take e as 60 mm. By substituting a, b, and e into Eq. (1), the minimum transmission angle is derived as

$$\gamma_{\min} = \arccos \frac{a + e}{b} = 47.6 > \gamma = 40^\circ \, .$$

The length of the serrated section is calculated as follows. The crankshaft AB rotates anticlockwise and clockwise, and the upper arm lifts from standstill to fall to switch the boom position.

From Fig. 2, the length of OC is

$$OC = OE + EC = \arccos \beta + \sqrt{b^2 - (e + a \sin \beta)^2}, \quad (15^\circ < \beta < 165^\circ) \, . \tag{5}$$

The values of a, b, and e are substituted into (5). The variation of length OC with angle β is shown in Fig. 2.

As can be seen from Fig. 2, when β equals 153°, length OC attains the minimum value of 116.45 mm; when β equals 15°, length OC attains the maximum value of 285.81 mm. In order to fix the position of the connecting rod, the travel segment is arranged in a zigzag shape. Therefore, the sawtooth segment has a horizontal distance of 100–300 mm.

3. Results

The stability of the picking-assist exoskeleton is simulated using ADAMS virtual prototype simulation software. A set of crank slider mechanisms is randomly designed for comparison with the optimized crank slider mechanism. The picking-assist exoskeleton is selected separately as the measurement object. A component fixing force is applied on the boom support plate to simulate the force that the boom lifts. Its action time is 0.2 s, and the duration of the exercise is 0.4 s.

The slider moves upward from standstill and then downward, ready to snap in the corresponding slot. Figures 3 and 4 show the curves of the slider velocity and angular velocity at the points of joints A, B, and C, respectively. As can be seen from these figures, curves of speed and angular speed of the optimized crank-slider mechanism are more stable than those of the unoptimized ones with few changes. Fluctuation is observed at the beginning of each curve because the slider in the rack starts to move to produce a smaller abrupt change. Because of the different sizes of the two crank-slider mechanisms, the trend of the two comparison curves is the same, and the second intersection of each curve with the X-axis is different. Fluctuations that occur in approximately 0.25 s are due to fluctuations in slider motion on the rack and crank motion perpendicular to the rack.

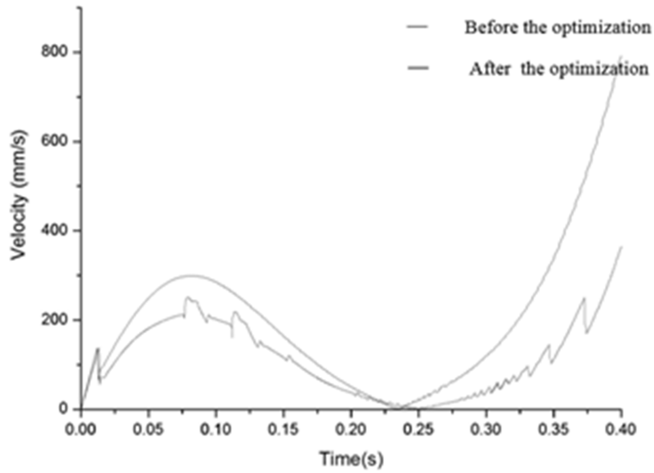

Fig. 3. Slider velocity curves before and after optimization

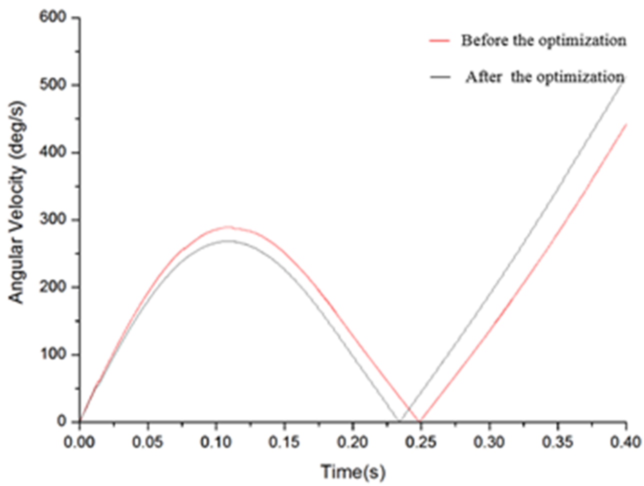

Fig. 4. Curves of angular velocity of joint A before and after optimization

4. Conclusion

In view of the work requirements of picking operations, an overall design scheme is proposed for a picking-assist exoskeleton. It achieves follow-up with the operator to meet their needs. According to the boom motion information, the size and rotation angle of the exoskeleton are calculated and optimized. A three-dimensional model is constructed based on these features. Finally, ADAMS is used to simulate the motion with a STEP function and to compare the effects of pre-optimization and post-optimization models, verifying the feasibility of the picking-assist exoskeleton for assisting in the work space to complete operations. The results of this study serve as a reference for establishing models for picking-assist exoskeletons, and can also provide theoretical model support for expanding the scope of application of the exoskeleton in agricultural production.

References

[1] A. Dag, I. Zipori, Y. Tugendhaft: *Mechanical harvesting of table olives: Harvest efficiency and fruit quality.* HortScience: A publication of the American Society for Horticultural Science *49* (2013), No. 1, 55–58.

[2] P. F. Croshaw: *Hardiman I Arm Test - Hardiman I Prototype Project.* PN (1969).

[3] B. J. Makinson: *Research and development prototype for machine augmentation of human strength and endurance: Hardiman I project.* The Company (1971).

[4] D. Zhang: *Study on the power assist exoskeleton system for upper limb driven by pneumatic pneumatic artificial muscles.* Doctoral Thesis, Zhejiang University (2014).

[5] A. M. Dollar, H. Herr: *Lower extremity exoskeletons and active orthoses: Challenges and State-of-the-Art.* IEEE Transactions on Robotics *24* (2008), No. 1, 144–158.

[6] E. Akdoğan, M. A. Adli: *The design and control of a therapeutic exercise robot for lower limb rehabilitation: Physiotherabot.* Mechatronics *21* (2011), No. 3, 509–522.

[7] J. C. Perry, J. Rosen, S. Burns: *Upper-limb powered exoskeleton design.* IEEE/ASME Transactions on Mechatronics *12* (2007), No. 4, 408–417.

Received October 12, 2017